

Delay-induced chaos with multifractal attractor in a traffic flow model

L. A. SAFONOV^{1,2}, E. TOMER¹, V. V. STRYGIN², Y. ASHKENAZY³ and S. HAVLIN¹

¹ *Minerva Center and Department of Physics, Bar-Ilan University
Ramat-Gan 52900, Israel*

² *Department of Applied Mathematics and Mechanics, Voronezh State University
Voronezh 394693, Russia*

³ *Center for Global Change Science, Massachusetts Institute of Technology
Cambridge, MA 02139, USA*

(received 18 April 2001; accepted in final form 26 October 2001)

PACS. 02.30.Ks – Delay and functional equations.

PACS. 05.45.Ac – Low-dimensional chaos.

PACS. 89.40.+k – Transportation.

Abstract. – We study the presence of chaos in a car-following traffic model based on a system of delay-differential equations. We find that for low and high values of cars density the system has a stable steady-state solution. Our results show that above a certain time delay and for intermediate density values the system passes to chaos following the Ruelle-Takens-Newhouse scenario (fixed point–limit cycles–two-tori–three-tori–chaos). Exponential decay of the power spectrum and non-integer correlation dimension suggest the existence of chaos. We find that the chaotic attractors are multifractal.

Traffic flow often exhibits irregular and complex behavior. It was observed experimentally (*e.g.*, [1]) that, although for low and high cars density the motion is relatively simple, for intermediate density values (in the so-called “synchronized flow phase” [1]) the motion is characterized by abrupt changes in cars velocities and flow flux. We study a model based on a system of delay-differential equations, which for sufficiently large delay and intermediate density values demonstrates complex behavior, attributed to the presence of chaos.

The presence of chaotic phenomena in traffic models has been reported in recent studies. Addison and Low [2] observed chaos in a single-lane car-following model in which a leading car has oscillating velocity. Nagatani [3] reported the presence of a chaotic jam phase in a lattice hydrodynamic model derived from the optimal velocity model [4].

Unlike the above models/studies, our model is based on a system of *autonomous* delay-differential equations, and the transition to chaos is possible only in the presence of delay (¹). We show that the system can pass to chaos via many similar routes and many different non-chaotic and chaotic attractors may coexist for the same parameter values. We also observe multifractality of the chaotic attractor, which is novel in traffic studies.

We generalize the model introduced and studied in [7–9] by introducing time delay in the driver’s reaction. The model is based on the assumption that N cars move in a single lane

(¹)Similarly to classical Mackey-Glass [5] and Ikeda [6] equations.

and the n -th car motion is described by the delay-differential equation

$$\frac{d^2x_n(t)}{dt^2} = A \left(1 - \frac{\Delta x_n^0(t-\tau)}{\Delta x_n(t-\tau)} \right) - \frac{Z^2(-\Delta v_n(t-\tau))}{2(\Delta x_n(t-\tau) - D)} - kZ(v_n(t-\tau) - v_{\text{per}}) + \eta, \quad (1)$$

where $n = 1, \dots, N$, x_n is the car's coordinate, v_n its velocity, A and k are sensitivity parameters, D is the minimal distance between consecutive cars, v_{per} the permitted velocity, T the safety time gap, $\Delta x_n^0 = v_n T + D$ the safety distance, $\Delta x_n = x_{n+1} - x_n$, $\Delta v_n = v_{n+1} - v_n$ and τ is time delay, η the random noise, uniformly distributed between $-\eta'$ and η' . The function Z is defined as $Z(x) = x$ for $x > 0$ and $Z(x) = 0$ for $x \leq 0$. In our computations we use the parameters values $v_{\text{per}} = 25(\text{m/s})$, $T = 2(\text{s})$, $D = 5(\text{m})$, $A = 3(\text{m/s}^2)$ and $k = 2(\text{s}^{-1})$, which are consistent with experimental observations. We assume that $N = 100$. The boundary conditions are periodic, *i.e.* $x_{N+1} = x_1 + L$, $v_{N+1} = v_1$, where L is the road length. The analysis of bifurcations, transition to chaos, and multifractality of chaotic attractors in this paper are performed assuming that $\eta' = 0$.

The first term in eq. (1) is dominant when the velocity difference between consecutive cars is relatively small. In this case the n -th car accelerates if $\Delta x_n > \Delta x_n^0$ and brakes if $\Delta x_n < \Delta x_n^0$. The second term plays an important role when $v_n \gg v_{n+1}$. A car getting close to a much slower car starts braking even if $\Delta x_n > \Delta x_n^0$. This term corresponds to the negative acceleration needed to reduce $|\Delta v_n|$ to 0 as $\Delta x_n \rightarrow D$. The dissipative third term is a repulsive force acting when the velocity exceeds the permitted velocity.

We have found in [9] that system (1) in variables $(\Delta x_n, v_n)$ without delay ($\tau = 0$) has many stable limit cycles. These cycles emerge after supercritical Hopf bifurcations (see, *e.g.*, [10]) with the density changing from high to intermediate values. They can be found by analytical approximation for densities close to bifurcation values and continued numerically as the density is decreased further.

Here we find that for sufficiently large delay the system behaves in a complex manner. We show, numerically, that the above-mentioned limit cycles may bifurcate into two-dimensional tori. With further change of density the tori bifurcate into three-dimensional tori, which are subsequently destroyed forming chaotic attractors. This scenario is known as Ruelle-Takens-Newhouse route to chaos [11] ⁽²⁾.

To study the transition to chaos we first consider the following solution of system (1):

$$v_n^0 = v^0 = \begin{cases} \frac{A(1-D\rho) + kv_{\text{per}}}{A\rho T + k}, & \rho \leq \frac{1}{D + Tv_{\text{per}}}, \\ \frac{1-D\rho}{\rho T}, & \rho > \frac{1}{D + Tv_{\text{per}}}, \end{cases} \quad x_n^0 = \frac{n-1}{\rho} + v^0 t, \quad (2)$$

where $\rho = N/L$ is the flow density. This solution corresponds to the homogeneous flow, in which all cars have the same velocity and spaces between neighboring cars are all equal. We introduce a new variable $\xi_n = \Delta x_n - 1/\rho$ in eq. (1). By this change of variables the homogeneous flow solution (2) is mapped to zero. Its stability can be analyzed using the linearization of eqs. (1):

$$\ddot{\xi}_n^0(t) = -p\xi_n^0(t-\tau) + q(\xi_{n+1}^0(t-\tau) - \xi_n^0(t-\tau)), \quad (3)$$

where $p = AT\rho + k$, $q = \frac{AT + kTv_{\text{per}} + kD}{AT\rho + k} \cdot A\rho^2$ if $\rho \leq \frac{1}{D + Tv_{\text{per}}}$ and $p = AT\rho$, $q = A\rho$ otherwise.

⁽²⁾The Ikeda equation [6] is a fundamental example of a delay-differential equation exhibiting the same scenario of transition to chaos.

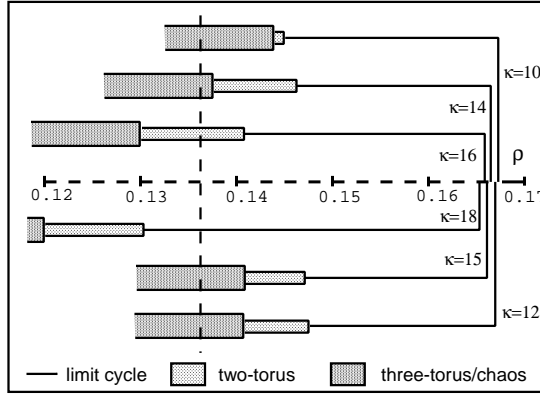


Fig. 1 – A schematic bifurcation diagram, showing transition to chaos from six different limit cycles. The figure shows that limit cycles, two-tori and chaotic attractors can coexist for the same parameter values (see the vertical dashed line).

Following [4, 7], we look for a solution of eqs. (3) in the form

$$\xi_n^0 = \exp[i\alpha_\kappa n + \lambda t], \tag{4}$$

where $\alpha_\kappa = \frac{2\pi}{N}\kappa$ ($\kappa = 0, \dots, N - 1$) and λ is a complex number. Substituting (4) into (3) we obtain a set of algebraic equations for λ :

$$\lambda^2 + [p\lambda - q(e^{i\alpha_\kappa} - 1)]e^{-\lambda\tau} = 0. \tag{5}$$

The solutions of eqs. (5) are the eigenvalues of system (3). One of these solutions (for $\kappa = 0$) is zero. The others have negative real part for sufficiently high and sufficiently low values of ρ , which indicates the stability of the homogeneous flow solution. As ρ decreases (increases), pairs of complex eigenvalues may cross the imaginary axis, causing the formation of small limit cycles (Hopf bifurcations).

We study the formation of limit cycles with the density decreasing from high to intermediate values. Let, for some $\rho = \rho_0$, eqs. (5) for some κ have a pair of purely imaginary solutions (a Hopf bifurcation point). For $\rho = \rho_0 - \varepsilon$ we find the newly born limit cycle in the form $\xi_n(t) \sim \varepsilon \xi_n^0(t)$, using an approximate technique similar to that used in [9] for the non-delay case. Obviously, the flow state corresponding to this limit cycle is a wave with the wavelength equal to L/κ (in length units) or N/κ (in number of cars).

After the small limit cycle for density close to the Hopf bifurcation value is found analytically, its global continuation is performed numerically in the following manner. For $\rho \approx \rho_0 - \varepsilon$ we take the analytically found approximate periodic solution as an initial condition and solve eqs. (1) numerically. After the solution has reached an attracting set, we decrease ρ with a small step and solve the equations numerically again, taking the results from the previous step as initial conditions. This procedure is iterated further. In this way we keep the track of the particular κ -cycle.

For the non-delay case [9] we have not found any other attracting sets than limit cycles. With a small delay the system’s behavior does not change qualitatively. For higher values of τ (above approximately 0.5 s) the cycles may undergo bifurcations leading to the transition to chaos.

A bifurcation diagram obtained from global continuation of six different limit cycles for $\tau = 0.59$ is sketched in fig. 1. The figure shows the transition from each of these cycles to

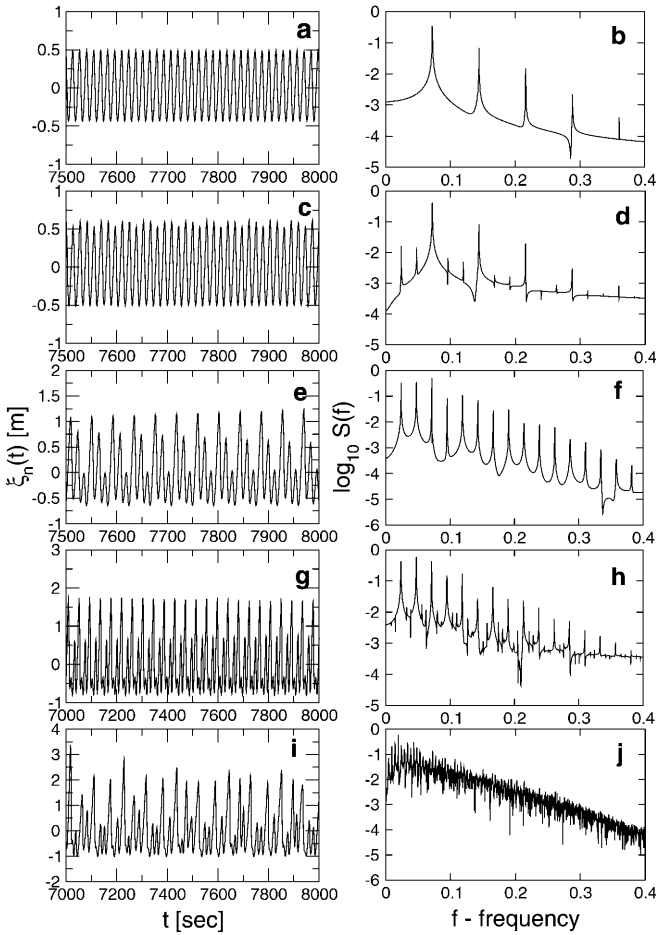


Fig. 2

Fig. 2 – Transition to chaos from the periodic solution with $\kappa = 15$ for $N = 100$ and $\tau = 0.59$. Left column: ξ_n for $n = 10$; right column: corresponding power spectra. a), b) $\rho = 0.1492$; c), d) $\rho = 0.1467$; e), f) $\rho = 0.1442$; g), h) $\rho = 0.1402$; i), j) $\rho = 0.1387$.

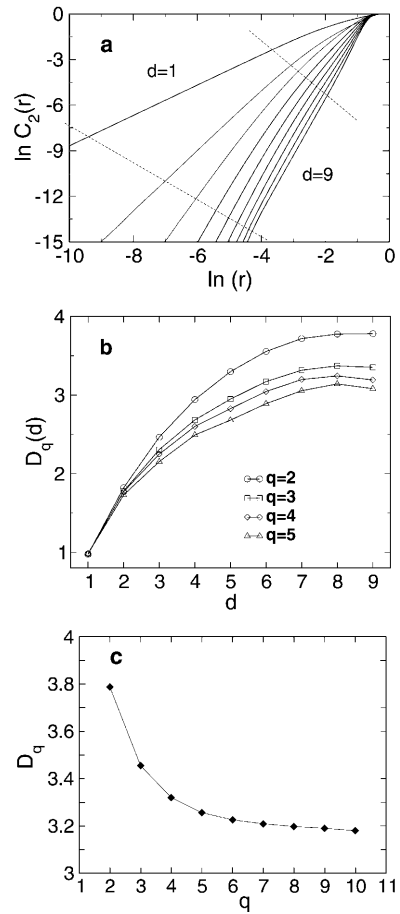


Fig. 3

Fig. 3 – a) Results of measurement of the correlation dimension D_2 . The parameter values are the same as in fig. 2i), j). The dashed lines indicate the range over which the slope for the dimension calculation was performed. b) Results of measurement of the generalized correlation dimension D_q for $q = 2, \dots, 5$ and $d = 1, \dots, 9$. c) D_q for $q = 2, \dots, 10$ and $d = 8$.

chaos via a two-torus phase. It is important to note that chaotic and non-chaotic attractors coexist for the same parameters values.

The transition to chaos from the cycle with $\kappa = 15$ is shown in more details in fig. 2. The cycle was formed after a Hopf bifurcation at $\rho \approx 0.1665$. Figures 2a), c), e), g) and i) show the dependence of ξ_n (for an arbitrarily chosen n) on t for different values of ρ . Presented in figs. 2b), d), f) and j) are the corresponding power spectra.

Figures 2c), d) depict the loss of stability by this cycle at $\rho \approx 0.1467$. It can be seen from fig. 2d) that a new independent frequency which is approximately three times smaller than the

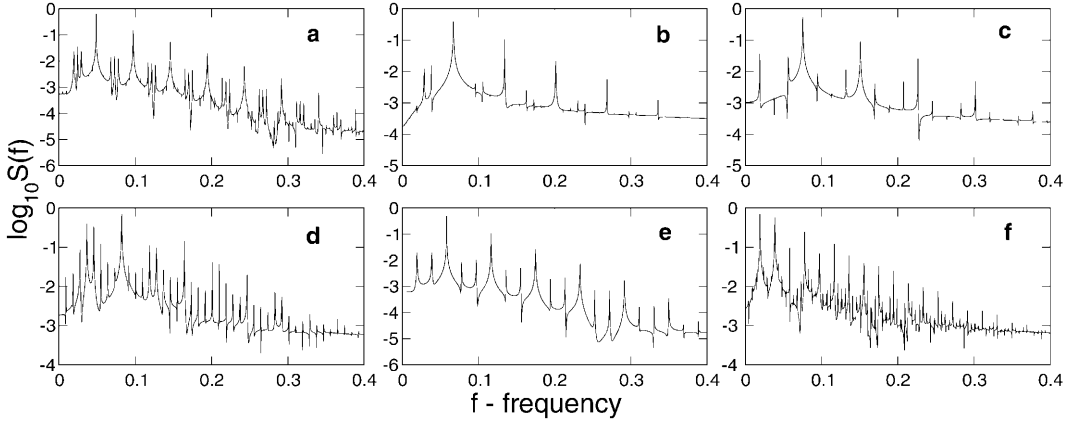


Fig. 4 – a)–e) Power spectra of the solutions originated from limit cycles with $\kappa = 10$ ($\rho = 0.1449$), 14 ($\rho = 0.1459$), 16 ($\rho = 0.1410$), 18 ($\rho = 0.1303$) and 12 ($\kappa = 0.1476$), respectively, immediately after the limit cycle→two-torus bifurcation. The ratio of the new frequency to the old one is close to a divisor of κ (10, 7, 4, 9 and 3, respectively). f) Power spectrum of the solution originated from the cycle with $\kappa = 12$ ($\rho = 0.1420$) after the two-torus→three-torus bifurcation. The frequencies ratio is also close to an integer.

original one appears. This indicates a bifurcation of a two-torus from the cycle. The system’s motion on the torus looks quasiperiodic (see fig. 2e), where the local maxima values change slightly from period to period).

As we continue to decrease ρ further we find that at $\rho \approx 0.1402$ one more independent frequency emerges, which is nearly three times smaller than the previous one. This is an indication of a bifurcation of a three-torus from the two-torus. The motion on the three-torus is shown in figs. 2g), h). This three-frequency quasiperiodic motion is observed only for a limited time interval, after which it becomes more complex. This might indicate that the system is driven to chaos by a small computational error according to the Ruelle-Takens theory [11].

With further decrease of density the motion becomes chaotic. The fully developed chaotic regime is shown in figs. 2i), j). The exponential decay of the power spectrum in fig. 2j) is an additional sign of chaotic behavior of our system. This decay can be associated with the sharp decrease of the autocorrelation function at large scale, which is characteristic to chaos [12]. Next, we measure the generalized correlation dimension [13] of a single-car time series, $\xi_n(t)$, using the algorithm proposed in [14]. We study the correlation function

$$C_q(r) = \left[\frac{1}{N} \sum_{i=1}^N \left[\frac{1}{N} \sum_{j=1}^N \Theta(r - |\mathbf{x}_i - \mathbf{x}_j|) \right]^{q-1} \right]^{\frac{1}{q-1}}, \quad (6)$$

where $\mathbf{x}_i = (\xi_n(t_i), \xi_n(t_i + \Delta t), \dots, \xi_n(t_i + (d-1)\Delta t))$ are d -dimensional vectors (d is called embedding dimension), Δt is the first zero of the time series autocorrelation function, and Θ is the Heaviside step function (see [13, 14] and references therein for more details). The correlation dimension D_q is defined by the relation $C_q(r) \sim r^{D_q}$. The plots of $C_2(r)$ for increasing embedding dimension ($d = 1, \dots, 9$) are shown in fig. 3a). With growing embedding dimension the curves converge to straight lines with the slope close to 3.8, which is the value of the correlation dimension D_2 . We repeat this calculation for increasing moments q and find that the generalized correlation dimension D_q decreases —this suggests that the system’s attractor is associated with many exponents and has multifractal properties (fig. 3b), c)).

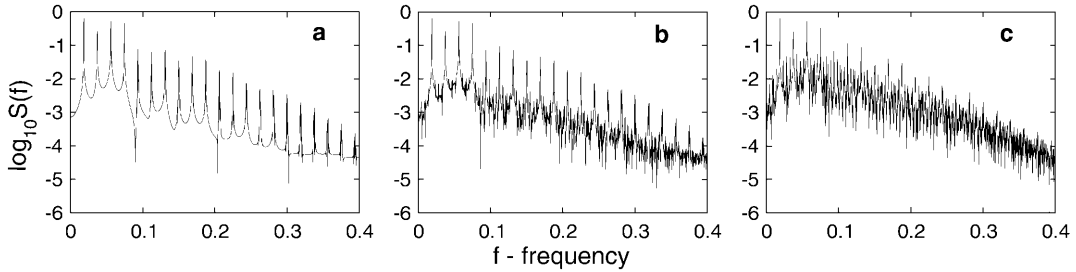


Fig. 5 – Power spectra of the single-car trajectories for $\kappa = 16$, $\rho = 0.135$, and $\eta' = 0$ (a), $\eta' = 0.0001$ (b), $\eta' = 0.001$ (c).

An additional sign for chaos is the existence of positive Lyapunov exponents. The Kaplan-Yorke conjecture connects the Lyapunov dimension D_L with the Lyapunov exponent spectrum by $D_L = j + \sum_{i=1}^j \lambda_i / |\lambda_{j+1}|$, where the Lyapunov exponents are sorted in decreasing order ($\lambda_1 > \lambda_2 > \dots > \lambda_n$) and j is defined by the conditions $\sum_{i=1}^j \lambda_i > 0$ and $\sum_{i=1}^{j+1} \lambda_i < 0$. Since $D_L \geq D_2$ [15], our system has at least one positive Lyapunov exponent.

A direct calculation of Lyapunov exponents (using the methods described in [16] and [17]) yields three positive Lyapunov exponents of order 10^{-4} . Because these exponents are small and close to each other, they cannot be used to accurately estimate D_L .

We performed similar studies of transition to chaos from cycles with several other κ 's. We observe that the transition follows the same scenario and found that the ratio of the old frequency to the new one at the limit cycle \rightarrow torus bifurcation is close to a divisor of the corresponding κ . For example, it is close to 10 for $\kappa = 10$ (fig. 4a)), 7 for $\kappa = 14$ (fig. 4b)), 4 for $\kappa = 16$ (fig. 4c)), 9 for $\kappa = 18$ (fig. 4d)) and 3 for $\kappa = 12$ (fig. 4e)). At the two-torus \rightarrow three-torus bifurcation the ratio between the new and the previous frequency is also close to an integer, which is different for different tori. For example, for $\kappa = 12$ this ratio is close to 4 (fig. 4f)), while for $\kappa = 15$ it is nearly 3 (fig. 2h)).

We found that the fine structures observed in the model and described above are robust to noise. Figure 5 shows the power spectra of a single car trajectory for $\kappa = 16$, $\rho = 0.135$, $\tau = 0.59$ (which corresponds to the two-torus phase) and different values of η' . Evidently, the quasiperiodic motion persists for noise levels under some threshold. Moreover, this regime continues coexisting with chaotic states which originated from cycles with other κ 's.

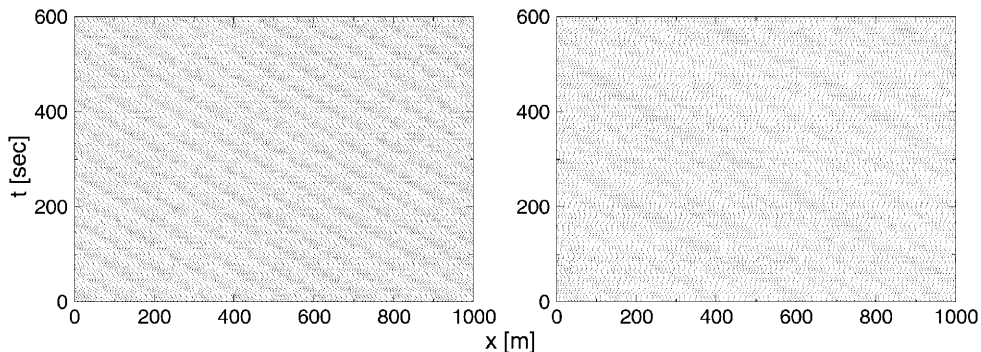


Fig. 6 – Space-time diagrams of the traffic flow for $\kappa = 10$ and $\rho = 0.1$. Left: $\tau = 0.4$ (a limit cycle); right: $\tau = 0.59$ (chaos). Each dot corresponds to a car.

Finally, we show that the incorporation of time delay into the model equations makes the model more realistic. For example, fig. 6 demonstrates the space-time diagrams of the model for $\kappa = 10$, $\rho = 0.1$ and two different values of τ . The left diagram corresponds to $\tau = 0.4$ and shows a periodic flow regime (limit cycle) with 10 jams moving backwards. The right diagram corresponds to $\tau = 0.59$ and shows the chaotic-regime traffic flow. The latter picture looks less ordered and more like what we can expect from real traffic observations.

In conclusion, we study a model of single-lane road traffic based on a system of autonomous delay-differential equations. We find that the presence of time delay accounts for the chaotic behavior of the system. The transition to chaos is found to follow the Ruelle-Takens-Newhouse scenario. The motion on the tori is periodic or quasiperiodic and many different tori and chaotic attractors may coexist for the same parameter values. We also observed that chaotic attractors of the system have multifractal properties.

* * *

We wish to thank I. DANA for useful comments. One of us (YA) thanks NIH/National Center for Research Resources (P41RR13622) and the NIA (AG14100) for partial support.

REFERENCES

- [1] KERNER B. S. and REHBORN H., *Phys. Rev. E*, **53** (1996) R4275; *Phys. Rev. Lett.*, **79** (1997) 4030; KERNER B. S., *Phys. World*, **12** (August) (1999) 25.
- [2] ADDISON P. S. and LOW D. J., *Chaos*, **8** (1998) 791; LOW D. J. and ADDISON P. S., *Nonlin. Dynam.*, **16** (1998) 127.
- [3] NAGATANI T., *Phys. Rev. E*, **60** (1999) 1535.
- [4] BANDO M., HASEBE K., NAKAYAMA A., SHIBATA A. and SUGIYAMA Y., *Phys. Rev. E*, **51** (1995) 1035; Y. SUGIYAMA, in *Proceedings of Workshop on Traffic and Granular Flow, Julich 1995*, edited by WOLF D. E., SCHRECKENBERG M. and BACHEM A. (World Scientific, Singapore) 1996.
- [5] MACKAY M. C. and GLASS L., *Science*, **197** (1977) 287.
- [6] IKEDA K. and MATSUMOTO K., *Physica D*, **29** (1987) 223.
- [7] TOMER E., SAFONOV L. and HAVLIN S., *Phys. Rev. Lett.*, **84** (2000) 382.
- [8] TOMER E., SAFONOV L. and HAVLIN S., *Traffic and Granular Flow '99: Social, Traffic and Granular Dynamics*, edited by HELBING D., HERRMANN H. J., SCHRECKENBERG M. and WOLF D. E. (Springer, Heidelberg/Berlin) 2000, p. 419.
- [9] SAFONOV L. A., TOMER E., STRYGIN V. V. and HAVLIN S., *Physica A*, **285** (2000) 147.
- [10] ALLIGOOD K. A., SAUER T. D. and YORKE J. A., *Chaos - An Introduction to Dynamical Systems* (Springer, New York) 1997.
- [11] NEWHOUSE S., RUELE D. and TAKENS F., *Commun. Math. Phys.*, **64** (1978) 35; RUELE D. and TAKENS F., *Commun. Math. Phys.*, **20** (1971) 167.
- [12] SCHUSTER H. G., *Deterministic Chaos: An Introduction* (VCH, Weinheim) 1995.
- [13] GRASSBERGER P. and PROCACCIA I., *Physica D*, **9** (1983) 189; PAWELZIK K. and SCHUSTER H. G., *Phys. Rev. A*, **35** (1987) 481.
- [14] ASHKENAZY Y., *Physica A*, **271** (1999) 427.
- [15] KAPLAN J. L. and YORKE J. A., in *Functional Differential Equations and Approximations of Fixed Points, Lect. Notes Math.*, Vol. **730**, edited by PEITGEN H.-O. and WALTHER H.-O. (Springer Verlag, Berlin) 1979.
- [16] ROSENSTEIN M. T., COLLINS J. J. and DE LUCA C. J., *Physica D*, **65** (1993) 117.
- [17] WOLF A., SWIFT J. B., SWINNEY H. L. and VASTANO A., *Physica D*, **16** (1985) 285.